

## Differentiation between Snake and Bee Venoms using Fluorescence Spectroscopy and Computational Approach

Alla M Hashkel<sup>1</sup>, Enas A Sadawe<sup>1</sup>, Asia Mohamed<sup>1</sup>, Nesren M Magel<sup>1</sup>, Ibrahim A Mrema<sup>1</sup>, Salah M Bensaber<sup>1</sup>, Fathi M Sherif<sup>2</sup>, Massaud Salem Maamar<sup>3</sup>, Amira Abdulhakim Elmaghrbi<sup>3</sup>, Anton Hermann<sup>4</sup> and Abdul M Gbaj<sup>1\*</sup>

<sup>1</sup>Department of Medicinal Chemistry, Faculty of Pharmacy, University of Tripoli, Libya

<sup>2</sup>Department of Pharmacology, Faculty of Pharmacy, University of Tripoli, Libya

<sup>3</sup>Zoology Department, Faculty of Science, Tripoli University, Libya

<sup>4</sup>Department of Biosciences, University of Salzburg, Salzburg, Austria

\*Corresponding Author: Abdul M Gbaj, Associate Professor of Genetics and Biochemistry, Department of Medicinal Chemistry, Faculty of Pharmacy, University of Tripoli, Libya.

Received: June 01, 2018; Published: June 30, 2018

### Abstract

Phospholipase A<sub>2</sub> (PLA<sub>2</sub>), represents a major venom component of snakes and bees and exhibits a broad range of biological effects including myotoxicity, neurotoxicity, hemolysis, cardiotoxicity, anticoagulant and antiplatelet activities. Melittin, is the main component and the major pain producing substance of honeybee venom. The aim of the present study was to differentiate between snake and bee venoms using aqueous olive leaf extract (AOLE) employing fluorescence techniques. Tryptophan, which is contained in both snake and bee venoms is fluorescent at UV wavelength and hence widely used as a tool to monitor conformational changes in proteins and to draw inferences regarding local structure and dynamics. Fluorescence spectroscopy and molecular modeling have been used to analyze enzyme activity in the absence and presence of AOLE and to verify potential binding of AOLE components to the enzyme. Changes in the fluorescence intensities with blue and red shifts were obtained with bee and snake venoms, respectively. Binding of AOLE constituents near the active site of the enzyme could be evidenced and possible modes of interaction are discussed. The fluorescence method used was rapid and sensitive and was able to differentiate between snake and bee venoms utilizing AOLE.

**Keywords:** PLA<sub>2</sub>; AOLE; Bee Venoms

### Abbreviations

PLA<sub>2</sub>: Phospholipase A<sub>2</sub>; AOLE: Aqueous Olive Leaf Extract

### Introduction

Libya and surrounding countries are inhabited by numerous venomous snakes of medical importance. Among them are the families *Viperidae*, *Hydrophiidae*, *Elapidae* and *Atractaspididae*. *Cerastes cerastes cerastes* mainly inhabits North Africa (Libya, Sudan, Algeria, Tunisia etc.), and is sympatric with another Asian species *Cerastes cerastes gasperettii* found in (Jordan, Iran, Palestine, and Iraq). Venoms from snakes within the family *Viperidae* are complex biochemical mixtures that function to immobilize the prey and initiate digestion. Envenomation by viperid and crotalid snakes is typically characterized by hemorrhage and necrosis that can cause lasting tissue damage [1] if the individual survives the predation. *Cerastes cerastes* venom contains many enzymes showing proteolytic activity and causes multiple kinds of intoxications [2]. The toxicities cause substantial physiopathological changes in the liver, skin and heart. Phospholipases A<sub>2</sub> (PLA<sub>2</sub>) from *Cerastes cerastes* for example, has been associated with numerous toxicities including neurotoxicity, nephrotoxicity, lung toxicity, hepatotoxicity, and cardiotoxicity [3-5]. The lethal effect of snake venom mainly results from its active ingredients such as phospholipase A<sub>2</sub> (PLA<sub>2</sub>). Phospholipid hydrolysis by PLA<sub>2</sub> releases arachidonic acid whose metabolism results in the formation of potentially toxic reactive oxygen species (ROS) and lipid peroxides [5,6]. The increase in the activity of liver enzymes indicating the damage of heart, liver and other organs could be attributed to the synergistic action of the venom components [2,5].

Hemorrhagic effects of snake venoms are commonly measured by irritation of the skin, a test developed by Kondo, *et al.* using laboratory animals such as rabbits, rats, or mice [7,8]. In other cases measurements of the hemoglobin content in muscle or skin tissue exposed to the venom were used [1]. Unfortunately, these methods require large numbers of animals, extensive training and expertise in the methodology and yields highly variable results. Fluorescent substrates have already been used successfully to quantify venom endopeptidase activities and might provide a technique to larger scale analysis required for comparative studies of venoms and prey resistance [9]. The aim of this work is to validate a rapid and sensitive fluorescence method that can differentiate between snake and bee venoms using AOLE. *Cerastes cerastes* (Viperidae) venom is barely toxic, although it is reported to be similar in venom toxicity of *Echis*. Envenomation typically causes haemorrhage, necrosis, swelling, haematuria, nausea, and vomiting. *C. cerastes* contains a high content of phospholipase A<sub>2</sub> which causes myotoxicity and cardiotoxicity [10]. Studies of venom from both *C. cerastes* and *C. vipera* showed a total of eight venom fractions, the most powerful of which has haemorrhagic activity. Venom yields vary, with ranges of 19 - 27 mg to 100 mg of dried venom being reported for venom toxicity [10,11]. The LD<sub>50</sub> values of 0.4 mg/kg were applied intravenous (IV) or 3.0 mg/kg subcutaneous (SC). The lethal dose for humans is 40 - 50 mg [12].

Honey bee venom is a mixture of enzymes and peptides, a colorless and bitter tasting liquid. Enzymes in the bee venom comprise phospholipase A<sub>2</sub>, phospholipase B, α-glucosidase, hyaluronidase and phosphatase. In addition, bee venom contains peptides such as apamin, melittin, mast cell degranulating peptide, adolapin, tertiapin, melittin F, secapin and cardiopep [13-16]. Tryptophan (Trp) which is present in phospholipase A<sub>2</sub> and melittin is a naturally occurring amino acid, which exhibits fluorescence emission properties that are dependent on the polarity of the local environment around the Trp side chain [17].

## Materials and Methods

All experiments were conducted in Tris buffer (0.01M Tris, 0.1M NaCl, at pH 7.4). Glass-distilled deionized water and analytical grade reagents were used throughout experiments. pH values of solutions were measured with a calibrated Jenway pH-meter model 3510 (Staffordshire, UK). All buffer solutions were filtered through Millipore filters (Millipore, UK) of 0.45 mm pore diameter.

**Absorbance spectra:** Absorbance spectra were measured on a Jenway UV-visible spectrophotometer, model 6505 (London, UK) using quartz cells of 1.00 cm path length. The UV-Vis absorbance spectra were recorded in the 200 - 500 nm range, and spectral bandwidth of 3.0 nm. For the final spectrum of each solution analyzed baseline subtraction of the buffer solution was performed. The protein content of venoms samples was determined by the spectrophotometric method of Markwell, *et al* [18]. Bovine serum albumin (BSA, Sigma) was used for standard assays.

**Fluorescence spectra:** Fluorescence emission and excitation spectra were measured using a Jasco FP-6200 spectrofluorometer (Tokyo, Japan) using fluorescence 4-sided quartz cuvettes of 1.00 cm path length. The automatic shutter-on function was used to minimize photo bleaching of the sample. The selected wavelength chosen provided aggregate excitation of tryptophan and tyrosine residues. The emission spectrum was corrected for background fluorescence of the buffer.

## Preparation of aqueous *Olea europaea* leaf extracts

Leaves of olive trees (*Olea europaea*) were collected from the Novellien zone, Tripoli Centre, Tripoli, Libya during April 2018. The leaves (5g) were cleaned and washed with distilled water and dried at a room temperature of 25°C for about 20 minutes. Dried leaves were grinded in a homogenizer (HO4A Edmund Buhler GmbH, UK) along with 15 ml of distilled water. The resulting aqueous solution was filtered using a Millipore filter (0.45 μm, GHD Acrodisc GF, UK).

## Venoms

Snake (*Cerastes cerastes*, *Macrovipera deserti*, *Echis pyramidum*) and bee (*A. m. scutellata*) venoms were extracted by manual stimulation and were obtained in liquid and semisolid forms, respectively, from the Zoology Department, Faculty of Science, Tripoli University (Libya) and stored at -20°C until use. Venoms were added to 2 ml of 0.01 M Tris, 0.1M NaCl at pH 7.4.

### Molecular docking

The 2D structures of AOLE constituents were drawn using ChemDraw Ultra (version 8.0, CambridgeSoft Com., USA). Chem3D Ultra was used to convert 2D structure into 3D and the energy was minimized using the semi-empirical AM1 method. Minimized energy to minimum RMS gradient of 0.100 was set in each iteration. All structures were saved as PDB file format for input to ADT. All AOLE constituents chemical structures were then saved in PDBQT file format to carry out docking in ADT. The crystal structures of bee-venom phospholipase A2 and the cobra-venom phospholipase A2 in a complex with a transition-state analogue were downloaded from the Protein Data Bank (<https://www.rcsb.org/structure/1POC>, <https://www.rcsb.org/structure/1POB>, respectively). In addition, the crystal structure of melittin was downloaded from the Protein Data Bank <http://www.rcsb.org/structure/2MLT>. The molecular docking of AOLE contents with both snake and bee phospholipase A2 and melittin were accomplished by AutoDock 4.2 software from the Scripps Research Institute (TSRI) (<http://autodock.scripps.edu/>). Firstly, the polar hydrogen atoms were added into phospholipase A2 and melittin molecules. Then, the partial atomic charges of phospholipase A2 and melittin and AOLE contents molecules were calculated using Kollman methods [19]. In the process of molecular docking, the grid maps of dimensions (62 Å X 62 Å X 62 Å) with a grid-point spacing of 0.376 Å and the grid box centered. The number of genetic algorithm runs and the number of evaluations was set to 100. All other parameters were default settings. Cluster analysis was performed on the results of docking by using a root mean square (RMS) tolerance of 2.0 Å, dependent on the binding free energy. Lastly, the dominating configuration of the binding complex of AOLE contents and phospholipase A2 and melittin proteins with minimum energy of binding determined.

### Results and Discussion

All snake venoms of *Cerastes cerastes*, *Macrovipera deserti* and *Echis pyramidum* behave similarly with AOLE using fluorescence spectroscopy; only the fluorescence results of *Cerastes cerastes* are shown in this work. The fluorescence spectrum shows a decrease of fluorescence intensity (Figure 1) of the snake venom due to addition of 100 µl of AOLE which could be related to various processes. It is well known that a decrease in fluorescence intensity can be caused by a range of molecular interactions such as molecular rearrangements, excited-state reactions, ground state complex formation, collisional quenching or energy transfer. The decrease in fluorescence emission intensity as shown in figure 1 was accompanied by a red shift of 7 nm of the maximum emission (343 nm to 350 nm) which may indicate that Trp residues buried in a hydrophobic environment have moved into a relatively polar environment consistent with earlier reports [20]. The decrease in fluorescence emission intensity (Figure 2) was accompanied by a blue shift of 24 nm of the maximum emission (352 to 328 nm) and this may indicate that binding of AOLE components may have accomplished a conformational change that moves Trp into a relatively more hydrophobic region.

Similar results report an increase in intrinsic tryptophan fluorescence and a blue shift of the maximum emission wavelength upon addition of MgATP to ArsA ATPase, indicating movement of Trp-159 into a relatively less polar environment [21]. The fluorescence of Phospholipases A<sub>2</sub> if excited at 280 nm is mainly due to the presence of a single tryptophan residue (Trp3) which is located on the surface of the enzyme molecule exposed to the environment [22].

The interaction between AOLE and the snake or bee venoms is not a concentration-dependent quenching of the fluorescence of the venom. Hence it is difficult to study fluorescence quenching which usually originates from collision between the fluorophore and the quencher (dynamic quenching) and/or is due to complex formation between the fluorophore and the quencher (static quenching) [23]. In addition, due to the red or blue shift of the fluorescence spectra, as seen in figure 1 and 2, it is difficult to determine the mechanism of interaction between fluorescence of both venoms and AOLE. Therefore, analysis by the Stern-Volmer equation to determine the quenching constant was not possible

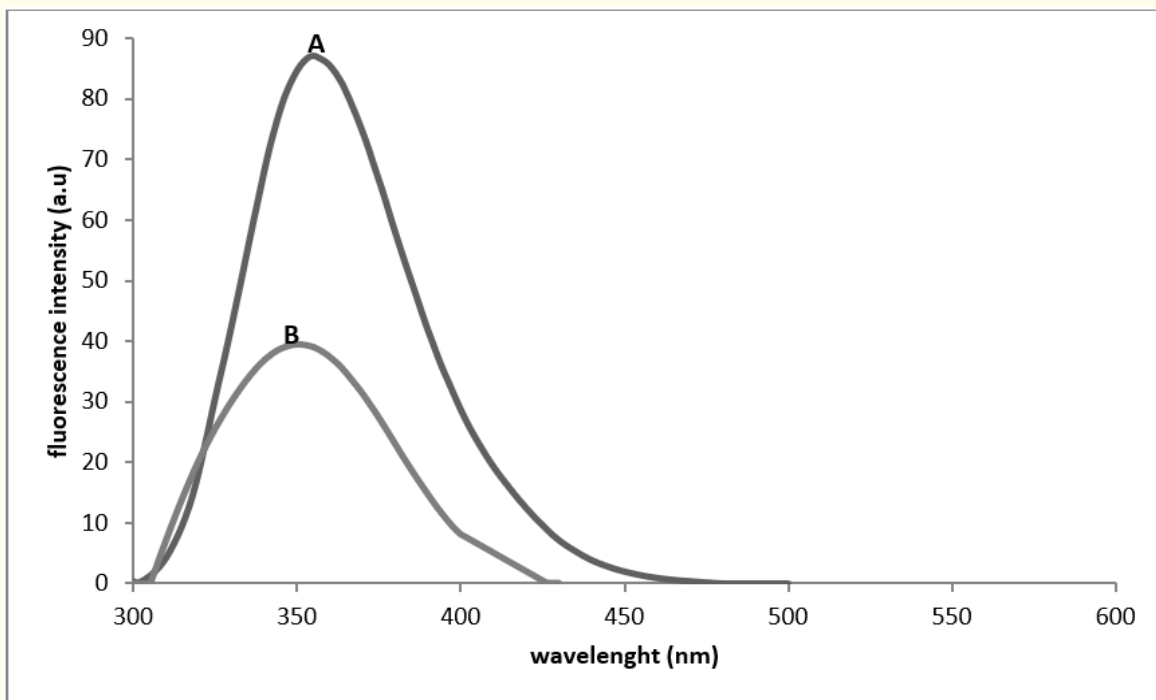


**Figure 1:** (A) Fluorescence perturbation of snake venom by addition of AOLE. Plot of fluorescence emission of snake venom (*Cerastes cerastes*) (24.6 µg/ml) vs wavelength from 288 - 540 nm using excitation of λ280 nm in 0.01 M Tris, 0.1 M NaCl at pH 7.4. (B) Plot of fluorescence emission of snake venom (*Cerastes cerastes*) (24.6 µg/ml) and 100 µl AOLE (5g/15 ml) vs wavelength from 288 - 540 nm using excitation of λ280 nm in 0.01 M Tris, 0.1 M NaCl at pH 7.4. Spectra were corrected for small background fluorescence contributions from the buffer solution and were scaled to visualize the shift..

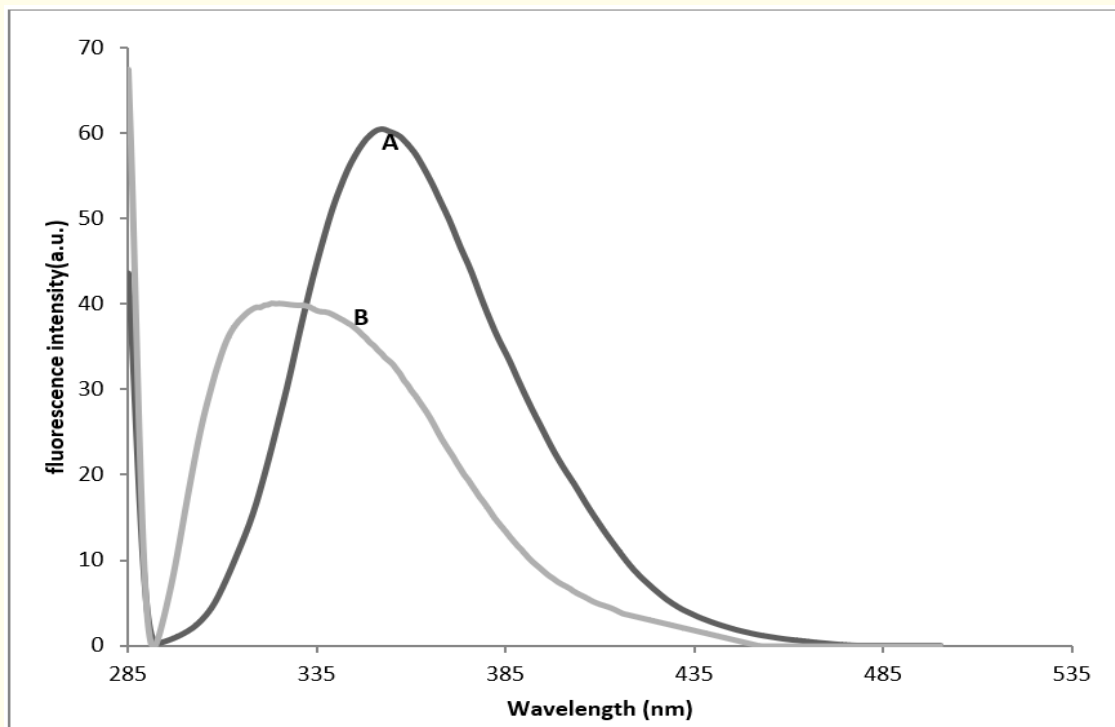


**Figure 2:** (A) Fluorescence perturbation of bee venom by addition of AOLE. Plot of fluorescence emission of bee venom (26 µg/ml, each 1 mg of dry venom contains 6.6 µg/ml protein) vs wavelength from 288 - 540 nm using excitation of λ280 nm in 0.01 M Tris, 0.1 M NaCl at pH 7.4. (B) Plot of fluorescence emission of bee venom (26 µg/ml) and 100 µl AOLE (5g/15 ml) vs wavelength from 288 - 540 nm using excitation of λ280 nm in 0.01 M Tris, 0.1 M NaCl at pH 7.4. Spectra were corrected for small background fluorescence contributions from buffer solution and were scaled to visualize the shift.

Solvent polarity and the local environment have profound effects on the spectral emission properties of fluorophores. The effect of solvent polarity is an important determinant of the Stokes shift, which is one of the earliest observations in fluorescence and was seen clearly in our experiments. Emission spectra are easily measured, resulting in numerous publications on emission spectra of fluorophores in different solvents and bound to proteins, membranes, DNA or RNA. One general use of solvent effects is to determine the polarity of the probe binding site at the macromolecule. This is accomplished by comparison of emission spectra and/or quantum yields if the fluorophore is bound to the macromolecule or dissolved in solvents of different polarity. However, there are many additional instances where solvent effects are used. We used them when the fluorescent bee and snake venoms bind to any component of AOLE. The binding was accompanied by a spectral shift or change in quantum yield due to the different environment for the bound fluorescence component. The fluorescence spectral changes can be used to measure the extent of binding between the fluorescent protein and the AOLE components. The effects of the environment on fluorescence spectra and quantum yields are complex and are due to several factors including: solvent polarity, viscosity, rate of solvent relaxation, probe conformational changes, rigidity of the local environment, internal charge transfer, proton transfer, excited state reactions, probe-probe interactions or changes in radiative and non-radiative decay rates. These multiple effects may offer chances to probe the local environment surrounding a fluorophore. However, environmental effects are usually complex and even solvent polarity cannot be described using a single theory. The Lippert-Mataga equation partially explains the effect of solvent polarity, but does not account for other effects such as hydrogen bonding to the fluorophore or internal charge transfer that depends on solvent polarity [24,25]. Emission spectra are seen to shift considerably to longer or shorter wavelengths as the solvent polarity changes upon addition of AOLE. The sensitivity to solvent polarity could be related to electron-donating or -accepting groups on tryptophan. In addition, the hydroxyl group of polyphenols in AOLE serves as electron donor and the carbonyl group on tryptophan as electron acceptors. This condition might help to understand the observed fluorescence changes in snake and bee venoms dissolved in AOLE. The high sensitivity to the solvent is due to a charge shift away from the hydroxyl groups in the excited state towards the electron acceptor. This results in a large dipole moment in the excited state. The dipole moment interacts with the polar solvent molecules to reduce the energy of the excited state and hence decreases fluorescence intensity.

### Tryptophan Fluorescence-Bee venom

Bee venom PLA<sub>2</sub> contains two tryptophan residues [26,27] one near the N-terminus, Trp-8 and one near the C-terminus, Trp-128. In addition it has 8 tyrosine residues distributed throughout the protein sequence. The fluorescence emission spectrum of the native protein ( $\lambda_{\text{max}} = 352 \text{ nm}$ ) showed that the Trp residues were in a moderately hydrophobic environment [26,27]. When the enzyme was treated with AOLE the fluorescence emission first decreased sharply and then declined progressively, undergoing a small, but detectable blue shift, figure 2. The simplest interpretation of these results is that the highly hydrophobic contents of the AOLE binds to the enzyme very rapidly, perturbing the environment of one of the tryptophan residues, and then undergoes a relatively slow reaction in which the AOLE components were transferred to an acceptor residue which leads to further perturbation of the tryptophan environment.

### Molecular docking analysis

Table 1 shows the energies of binding of the AOLE contents with bee and venom phospholipase A2 and melittin obtained by using molecular docking strategy.

Molecular docking of AOLE contents with phospholipase A2 and melittin were performed using AutoDock 4.2 to investigate the binding mode of AOLE contents with phospholipase A2 and melittin and to obtain information about the interaction forces between AOLE contents and phospholipase A2 and melittin. AOLE which consists of flexible molecules was docked to two types of rigid phospholipase A2 and melittin proteins to obtain the preferential binding site(s) of AOLE to phospholipase A2 and melittin. The molecular docking results are shown in table 1.

Our modeling study indicates substantial interactions between AOLE contents and bee and snake PLA<sub>2</sub>. The docking binding energies are shown in table 1. For example, apigenin (an AOLE component) in case of snake PLA<sub>2</sub> was able to form hydrogen bonds with the residues Gly29, Leu249, Tyr27, Asp48 and Tyr63 of the enzyme, pi-pi stacking with the residue Phe5, Phe5, His47 and His47 and Pi-alkyl interaction with the residue Leu2. In addition, the molecular docking results indicate that other amino acid residues are involved in the interactions with AOLE contents. Similar binding energies of docking were obtained using AOLE with bee PLA<sub>2</sub> as shown in table 1. For

AOLE components		Bee Phospholipase a2 1POC	Snake Phospholipase a2 1POB	Melittin Mmdp
Structure	Ligand Pdb symbols	Binding Energy	Binding Energy	Binding Energy
5-caffeoylquinic acid	1d	-6.07	-3.11	-3.11
Cyanidine-3-glucoside	2d	-7.65	-4.23	-4.23
Demethyloleuropein	3d	-6.27	-3.4	-3.4
3,4-DHPEA-EDA	4d	-6.11	-2.27	-2.27
Hesperidin	5d	-7.62	-4.42	-4.42
Luteolin	8d	-7.83	-4.38	-4.38
Quercetin	9d	-7.46	-3.94	-3.94
Verbascoside	10d	-6.44	-2.07	-2.07
Nuzhenide	11d	-5.77	-1.56	-1.56
Protocatechuic acid	12d	-4.51	-4.38	-4.38
4-hydroxybenzoic acid	13d	-4.24	-3.93	-3.93
Hydroxytyrosol	14d	-5	-3.22	-3.22
Ferulic acid	16d	-5.05	-5.19	-5.19
Elenoic acid	17d	-6.02	-5.39	-5.39
Syringic acid	19d	-4.74	-4.2	-4.2
Vanillic acid	20d	-4.56	-4.17	-4.17
Sinapic acid	21d	-5.27	-3.97	-3.97
Tyrosol	22d	-4.88	-3.09	-3.09
Rutin	23d	-7.88	-3.95	-3.95
Oleuropein aglycon	24d	-6.29	-2.66	-2.66
p-Coumaric acid	25d	-5.12	-4.27	-4.27
O-coumaric acid	26d	-5.57	-4.71	-4.71
Caffeic acid	27d	-5.29	-4.47	-4.47
Cinnamic acid	28d	-5.02	-4.51	-4.51
Oleuroside	29d	-6.71	-2.52	-2.52
Ligstroside	30d	-7.54	-3.26	-3.26
Homoorientin	31d	-7.35	-4.77	-4.77
Apigenin	32d	-8.14	-4.22	-4.22
Catachin	cat	-7.74	-4.07	-4.07
L- L-O-octyl-2-heptylphospho- nyl-sn- glycerol-3-phosphoetha- nolamine (inhibitor)	Gel	-2.45	n -3.38	None

**Table 1:** Various energies in the binding process of AOLE contents with bee and venom phospholipase A2 and melittin obtained from molecular docking. The unit of all energies was kJ/mol.

<sup>a</sup> ΔG is the free binding energy change in the binding process (Kcal/mole)

example the AOLE component apigenin in case of bee PLA2 was able to form hydrogen bonds with the residues Phe82, His34 (two bonds) and Asp35 and Tyr57 of the enzyme, as well as pi-pi stacking with the residue Tyr87, Pi-alkyl interaction with the residue Cys8, Met86 and pi-sigma interaction with the residue Val83. The interactions of AOLE components (which were mainly polyphenolic components) obtained are in consistency with previous studies reporting that polyphenolic secondary metabolites are able to inhibit PLA<sub>2</sub> [28]. For example quercetin, kaempferol, galangin, naringenin, artemetin and other flavonoids can inhibit toxins from snake venom. They found that flavonoids usually exert their inhibitory effect through hydrophobic interactions with A and B rings and aromatic or hydrophobic amino

acid residues in the protein [29-31]. In addition, another research group found that Ar-turmerone which is a phenolic compound isolated from the *Curcuma longa* (Zingiberaceae) plant has a strong inhibitory effect against hemorrhage and lethality caused by *B. jararaca* and *C. d. terrificus* snake venom. The effect was attributed to the interaction with PLA<sub>2</sub> [32]. It has been also reported that 4-nerolidylcatechol (a hydroxylated phenolic compound) - an extract from *Piper umbellatum* and *P. peltatum* (Piperaceae) - is able to inhibit the myotoxic activities of PLA<sub>2</sub>s [33] and is able to interact and inhibit the function of PLA<sub>2</sub>s. Araya and Lomonte [34] found that caffeic acid which is one of the components of AOLE, can interact with proteins via hydrogen bonds, inhibiting enzyme function and acting as antidote. They found that strong interactions may cause conformational changes in the protein structure [34,35]. The interaction of caffeic acid with snake venoms were confirmed by Shimabuku and collaborators [36] who crystallized PrTX-I (basic Lys49-PLA<sub>2</sub> from *B. pirajai* snake venom) in the presence of the inhibitor caffeic acid. The electron-density map clearly signifies the presence of three caffeic acid molecules interacting with the C-terminus of the protein. The changes of fluorescence emission intensity and fluorescence shifts (blue and red) in which the formation of the system was formed by sequential addition of aliquots of Tris buffer, snake and bee venoms and finally AOLE (Figure 1, 2) confirms interaction obtained by the modeling studies.

The docking binding energies obtained from AOLE interacting with bee-melittin as shown in table 1 was due to the formation of hydrogen bonds with the residues Lys21 (three bonds), Ser18, and Leu9 of the enzyme, and pi-sigma interaction with the residue Ile17. In addition, the molecular docking results showed that the residues Ile17 (two bonds), Pro14 (two bonds), and Ile13 are involved in the pi-alkyl interactions with apigenin. Results provided by Chatterjee and Mukhopadhyay [37] reported that melittin interacts with ganglioside GM1 which is consistent with our findings and were confirmed by different techniques including steady-state fluorescence, molecular modeling and proton NMR spectroscopy [37]. They found that in the presence of GM1 the emission maximum of melittin was blue shifted and fluorescence quenching efficiencies of iodide and acrylamide were substantially reduced, indicating shielding of tryptophan of melittin from the aqueous environment. In their study with the aid of molecular modeling they confirm a melittin-GM1 complex with a N-terminal hydrophobic stretch of melittin connected through the ceramide tail and C-terminal hydrophilic end of melittin encompassing constructive electrostatic interaction with the carbohydrate head group of GM1 [37].

## Conclusion

Changes in fluorescence spectra indicate that the occupation of AOLE component binding sites cause conformational modifications of Phospholipase A<sub>2</sub> and melittin. The observed red-shift in the emission maximum suggests that the conformational change increases the exposure of at least one tryptophan residue to the solvent. As expected, the effect is immediate when induced by addition of AOLE components. Of the two Trp residues of bee PLA<sub>2</sub>, Trp-8 is located at a relatively internal hydrophobic environment near the active site, whilst Trp-128 is in a less compact region of the protein with a lower density of hydrophobic residues. Hence, Trp-8 is the more likely source of the observed changes. It is of interest to note that bee PLA<sub>2</sub> interacting with AOLE components gives significantly larger fluorescence changes compared to the snake venom suggesting that the two adjacent Trp residues could be involved. Evidence presented here shows that activation of PLA<sub>2</sub> is based on conformational modifications associated with occupation of a hydrophobic site on PLA<sub>2</sub>. In further studies using the fluorescence technique we will investigate the relationship between structural changes in the bee and snake venoms.

## Bibliography

1. de Roodt AR., et al. "A comparison of different methods to assess the hemorrhagic activity of Bothrops venoms". *Toxicon* 38.6 (2000): 865-873.
2. Mohamed AH., et al. "Toxic fractions of Cerastes cerastes venom". *Japanese Journal of Medical Science and Biology* 30.4 (1977): 205-207.
3. Siddiqi AR., et al. "Characterization of phospholipase A2 from the venom of Horned viper (Cerastes cerastes)". *FEBS Letters* 278.1 (1991): 14-16.
4. Gasanov SE., et al. "Phospholipase A2 and cobra venom cytotoxin Vc5 interactions and membrane structure". *General Physiology and Biophysics* 14.2 (1995): 107-123.
5. Alzahaby M., et al. "Some pharmacological studies on the effects of Cerastes vipera (Sahara sand viper) snake venom". *Toxicon* 33.10 (1995): 1299-1311.

6. Cavalcante WLG., *et al.* "Neuromuscular paralysis by the basic phospholipase A2 subunit of crotoxin from *Crotalus durissus terrificus* snake venom needs its acid chaperone to concurrently inhibit acetylcholine release and produce muscle blockage". *Toxicology and Applied Pharmacology* 334 (2017): 8-17.
7. Pradhan S., *et al.* "Development of passive haemagglutination (PHA) and haemagglutination inhibition (HAI) technique for potency estimation of Cobra Antisnake Venom Serum (ASVS)". *Biologicals* 35.3 (2007): 155-160.
8. Theakston RD and Reid HA. "Development of simple standard assay procedures for the characterization of snake venom". *Bulletin of the World Health Organization* 61.6 (1983): 949-956.
9. Gasparello-Clemente E and Silveira PF. "Fluorometric assay using naphthylamide substrates for assessing novel venom peptidase activities". *Toxicon* 40.11 (2002): 1617-1626.
10. Kebir-Chelghoum H and Laraba-Djebari F. "Cytotoxicity of *Cerastes cerastes* snake venom: Involvement of imbalanced redox status". *Acta Tropica* 173 (2017): 116-124.
11. Reid HA. "Epidemiology of sea-snake bites". *Journal of Tropical Medicine and Hygiene* 78.5 (1975): 106-113.
12. Fonger GC., *et al.* "Venoms and antivenoms: North American poisonous scorpion, snake, and spider information is now in the National Library of Medicine's Hazardous Substances Data Bank". *Clinical Toxicology* 53.1 (2015): 74.
13. Fischer FG and Neumann WP. "[The venom of the honeybee. III. On the chemical knowledge of the principle active constituent (melittin)]". *Biochemische Zeitschrift* 335 (1961): 51-61.
14. Hartter P. "[Basic peptides in bee venom, III. Synthesis of peptide fragments from the sequence of the mast-cell-degranulating peptide (author's transl)]". *Hoppe-Seyler's Zeitschrift Fur Physiologische Chemie* 358.3 (1977): 331-337.
15. Shipolini RA., *et al.* "Phospholipase A from bee venom". *European Journal of Biochemistry* 20.4 (1971): 459-468.
16. Orlov BN., *et al.* "[Chemistry and pharmacology of bee venom (a review of the literature)]". *Farmakologiya I Toksikologiya* 41.3 (1978): 358-369.
17. Kamceva T., *et al.* "Inhibitory effect of platinum and ruthenium bipyridyl complexes on porcine pancreatic phospholipase A2". *Metalomics* 3.10 (2011): 1056-1063.
18. Markwell MA., *et al.* "A modification of the Lowry procedure to simplify protein determination in membrane and lipoprotein samples". *Analytical Biochemistry* 87.1 (1978): 206-210.
19. Tiwari R., *et al.* "Carborane clusters in computational drug design: a comparative docking evaluation using AutoDock, FlexX, Glide, and Surflex". *Journal of Chemical Information and Modeling* 49.6 (2009): 1581-1589.
20. Kenoth R., *et al.* "Structural determination and tryptophan fluorescence of heterokaryon incompatibility C2 protein (HET-C2), a fungal glycolipid transfer protein (GLTP), provide novel insights into glycolipid specificity and membrane interaction by the GLTP fold". *Journal of Biological Chemistry* 285.17 (2010): 13066-13078.
21. Zhou T and Rosen BP. "Tryptophan fluorescence reports nucleotide-induced conformational changes in a domain of the ArsA ATPase". *Journal of Biological Chemistry* 272.32 (1997): 19731-19737.
22. Cunningham TJ., *et al.* "Product inhibition of secreted phospholipase A2 may explain lysophosphatidylcholines' unexpected therapeutic properties". *Journal of Inflammation* 5 (2008): 17.
23. Khot MS., *et al.* "Spectrofluorimetric determination of 5-fluorouracil by fluorescence quenching of 9-anthracenecarboxylic acid". *Spectrochimica Acta Part A: Molecular and Biomolecular Spectroscopy* 77.1 (2010): 82-86.
24. Snitsarev V., *et al.* "The spectral properties of (-)-epigallocatechin 3-O-gallate (EGCG) fluorescence in different solvents: dependence on solvent polarity". *PLoS One* 8.11 (2013): e79834.
25. Gong Y., *et al.* "Photophysical properties of photoactive molecules with conjugated push-pull structures". *Journal of Physical Chemistry A* 111.26 (2007): 5806-5812.



26. Kuchler K., *et al.* "Analysis of the cDNA for phospholipase A2 from honeybee venom glands. The deduced amino acid sequence reveals homology to the corresponding vertebrate enzymes". *European Journal of Biochemistry* 184.1 (1989): 249-254.
27. Chang ZY., *et al.* "Deduced amino acid sequence of Escherichia coli adenosine deaminase reveals evolutionarily conserved amino acid residues: implications for catalytic function". *Biochemistry* 30.8 (1991): 2273-2280.
28. Cotrim CA., *et al.* "Quercetin as an inhibitor of snake venom secretory phospholipase A2". *Chemico-Biological Interactions* 189.1-2 (2011): 9-16.
29. Ticli FK., *et al.* "Rosmarinic acid, a new snake venom phospholipase A2 inhibitor from Cordia verbenacea (Boraginaceae): antiserum action potentiation and molecular interaction". *Toxicon* 46.3 (2005): 318-327.
30. Soares AM., *et al.* "Medicinal plants with inhibitory properties against snake venoms". *Current Medicinal Chemistry* 12.22 (2005): 2625-2641.
31. Lattig J., *et al.* "Mechanism of inhibition of human secretory phospholipase A2 by flavonoids: rationale for lead design". *Journal of Computer-Aided Molecular Design* 21.8 (2007): 473-483.
32. Ferreira LA., *et al.* "Antivenom and biological effects of ar-turmerone isolated from Curcuma longa (Zingiberaceae)". *Toxicon* 30.10 (1992): 1211-1218.
33. Nunez V., *et al.* "Inhibitory effects of Piper umbellatum and Piper peltatum extracts towards myotoxic phospholipases A2 from Bothrops snake venoms: isolation of 4-nerolidylcatechol as active principle". *Phytochemistry* 66.9 (2005): 1017-1025.
34. Araya C and Lomonte B. "Antitumor effects of cationic synthetic peptides derived from Lys49 phospholipase A2 homologues of snake venoms". *Cell Biology International* 31.3 (2007): 263-268.
35. Lomonte B., *et al.* "Synthetic peptides derived from the C-terminal region of Lys49 phospholipase A2 homologues from viperidae snake venoms: biomimetic activities and potential applications". *Current Pharmaceutical Design* 16.28 (2010): 3224-3230.
36. Shimabuku PS., *et al.* "Crystallization and preliminary X-ray diffraction analysis of a Lys49-phospholipase A2 complexed with caffeic acid, a molecule with inhibitory properties against snake venoms". *Acta Crystallographica. Section F, Structural Biology and Crystalization Communications* 67.2 (2011): 249-252.
37. Chatterjee C and Mukhopadhyay C. "Melittin-GM1 interaction: a model for a side-by-side complex". *Biochemical and Biophysical Research Communications* 292.2 (2002): 579-585.

**Volume 6 Issue 7 July 2018**

**©All rights reserved by Abdul M Gbaj., *et al.***